The Jahn-Teller effect in the electron momentum spectroscopy of ammonia

J. S. Zhu, Y. R. Miao, J. K. Deng, and C. G. Ning

Citation: J. Chem. Phys. **137**, 174305 (2012); doi: 10.1063/1.4766202
View online: http://dx.doi.org/10.1063/1.4766202
View Table of Contents: http://jcp.aip.org/resource/1/JCPSA6/v137/i17
Published by the American Institute of Physics.

The Jahn-Teller effect in the electron momentum spectroscopy of ammonia

J. S. Zhu, Y. R. Miao, J. K. Deng, and C. G. Ning[a)]
State Key Laboratory of Low-Dimensional Quantum Physics, Department of Physics, Tsinghua University, Beijing 100084, China

(Received 8 August 2012; accepted 22 October 2012; published online 7 November 2012)

The $1e$ and $3a_1$ bands of the ammonia molecule have been studied using the high-resolution electron momentum spectroscopy at impact energies of 1200 and 600 eV. Several slices of $1e$ and $3a_1$ bands in the different binding energy ranges were selected, and their electron-momentum distributions were carefully compared. The discernable difference among the distributions of the selected slices of the $1e$ band shows that the Jahn-Teller effect indeed influences the electron momentum distribution of the $1e$ orbital of ammonia. © *2012 American Institute of Physics*. [http://dx.doi.org/10.1063/1.4766202]

I. INTRODUCTION

The Jahn-Teller effect of ammonia (NH_3) molecule, a textbook example for investigating vibronic coupling effect, has been studied for many years.[1–10] Photoelectron spectra (PES) of ammonia have clearly shown that the $1e$ band has a non-symmetric irregular profile.[1,11–19] Woywod *et al.* investigated the spectroscopic and dynamic aspects of Jahn-Teller and pseudo-Jahn-Teller interactions in NH_3^+. Their theoretical simulation of the vibronic structures of $1e$ band agreed with the PES very well.[9]

Electron momentum spectroscopy (EMS),[20–22] based on the kinetic complete $(e, 2e)$ reaction, is a powerful tool to investigate the electronic structures of atoms and molecules. It can measure the binding energy spectra and the electron momentum distributions for each orbital at the same time. Compared with the PES, EMS can provide the direct information about the vibronic effect on the electronic wavefunction by measuring the electron momentum distribution. Recently, Chen and co-workers reported the electron momentum spectroscopy study of Jahn-Teller effect of cyclopropane, which showed its influence on the electron-momentum distribution due to the geometry change.[23]

The electronic structure of ammonia has been investigated using the EMS method several times. However, the previous EMS studies mainly focused on the comparison of the experimental electron-momentum distributions and the theoretical calculations.[24–27] The Jahn-Teller effect was not investigated due to the low detection efficiency and the low energy resolution of the spectrometers at that time. In the present work, we use our high-efficiency and high-resolution spectrometer to examine if there is any dependence of the electron momentum distribution on the vibrational structure in the $3a_1$ and $1e$ orbital transitions. Several slices in the energy-momentum intensity map were selected and carefully compared for revealing the Jahn-Teller effect.

II. THEORETICAL AND EXPERIMENTAL METHODS

The details of our high resolution EMS spectrometer have been reported previously.[28–30] Therefore, only a brief description is given here. A specially designed electron gun, which has a barium oxide cathode working at a lower temperature than the generic tungsten filament, generates a collimated electron beam with a lower energy spread and a lower divergence angle. Under the symmetric non-coplanar geometry, the target atom or molecule is ionized by the high energy electron impact. The scattered and the knocked-out electrons are analyzed and coincidently detected with nearly equal kinetic energies and equal polar angles θ ($\theta_1 = \theta_2 = 45^\circ$) by a double toroidal energy analyzer and two position sensitive detectors. The momentum of the electron before being knocked out from the molecule is determined through the azimuthal angle ϕ between the two outgoing electrons:

$$p = \left[(2p_1\cos\theta - p_0)^2 + 4p_1^2\sin^2\theta\sin^2\left(\frac{\phi}{2}\right)\right]^{\frac{1}{2}}, \qquad (1)$$

where p_0 and p_1 are the momenta of the incident and the outgoing electron, respectively. With the standard calibration run for the Ar $3p$ orbital, the energy resolution was measured as $\Delta E = 0.7$ eV (full width at half maximum, FWHM) at the impact energy of 1200 eV. The azimuthal angle resolution is $\Delta\phi = \pm 0.84^\circ$ (one standard deviation) and the polar acceptance angle is $\Delta\theta = \pm 0.53^\circ$.[30]

Under the condition of high impact energy and high momentum transfer, the plane wave impulse approximation (PWIA) can be used for calculating the differential cross section of $(e, 2e)$ reaction. With the further target Kohn-Sham approximation, the differential cross section has a very simple and concise form for the randomly oriented gas-phase target atoms or molecules:[22]

$$\sigma_{\mathrm{EMS}} \propto \int d\Omega \left|\psi_j^{\mathrm{KS}}(p)\right|^2, \qquad (2)$$

where $\psi_j^{\mathrm{KS}}(p)$ is the jth Kohn-Sham molecular orbital in the momentum space and $\int d\Omega$ stands for the spherical average for the random orientation of molecules.

The neutral ammonia molecule has a pyramidal conformation with a C_{3v} symmetry. Its electronic orbital configuration of the ground state can be written as $(1a_1)^2(2a_1)^2(1e)^4(3a_1)^2$. According to the high resolution photoelectron spectra of NH_3,[19] the $1e$ band has a very broad width of 4.0 eV and there is nearly no resolved vibrational

a)ningcg@tsinghua.edu.cn.

structure due to the Jahn-Teller interactions. Three slices in the energy-momentum density map of the 1*e* band were selected to investigate the Jahn-Teller effect on the electron-momentum distributions. Compared with the congested and irregular structures of the 1*e* band, in the high resolution PES the $3a_1$ band has a clearly resolved vibrational structure due to the strong excitation of the umbrella mode ν_2, which is the consequence of the transition from a pyramidal to a planar equilibrium geometry upon ionization. The vibrational broadening of the $3a_1$ orbital is about 1.5 eV,[19] and two slices were selected for investigating the vibronic effects of NH_3^+ on the electron-momentum distribution.

III. RESULTS AND DISCUSSION

The observed momentum-density map of NH_3 under the impact energy of 1200 eV is shown in Fig. 1(a). The experiment was also conducted at 600 eV for checking the validity of PWIA. The binding energy spectrum in Fig. 1(b) was obtained by summing over all the azimuthal angles. The $3a_1$ orbital which is centered at 10.9 eV has a symmetric shape, while the 1*e* band is non-symmetric, which is consistent with the PES results.[1,11–19] In the binding energy spectrum there are five selected slices shaded with different colors. The energy ranges for the two slices of $3a_1$ band are 10.1−10.7 eV and 11.1−11.7 eV. The ranges of 15.1−15.9 eV, 16.1−16.9 eV, and 17.1−17.9 eV correspond to the three slices of 1*e* band. All of these slices have relative high counts (>8000) to ensure the statistical accuracy.

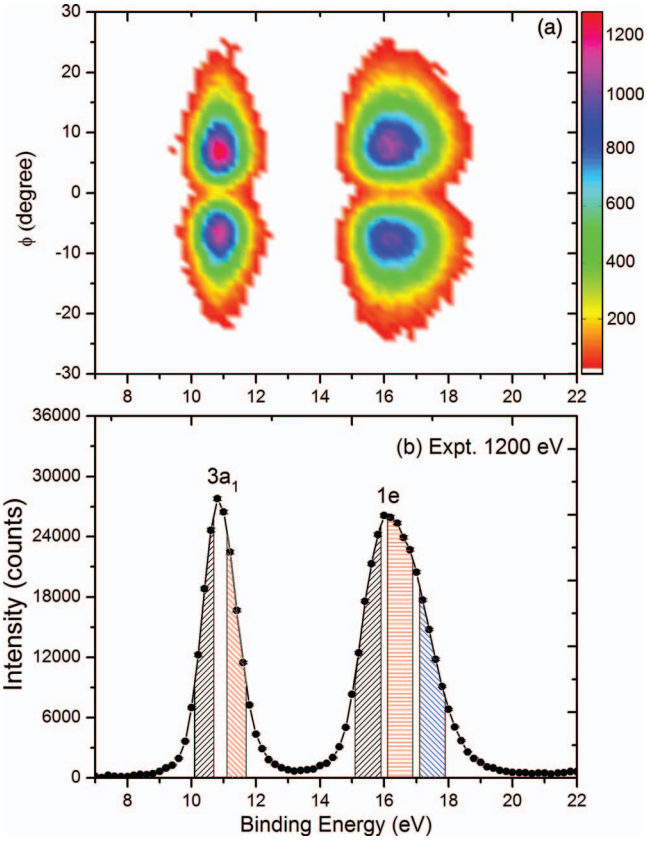

FIG. 1. Binding energy spectra of NH_3. (a) Momentum-energy density map of NH_3 at the impact energy of 1200 eV plus the binding energies. The intensity scale is shown by the color bar. (b) Experimental binding energy spectrum summed over all azimuthal angles. The five shaded areas under the curve are the selected slices of $3a_1$ and 1*e* bands for investigating the Jahn-Teller effect.

The electron-momentum distributions for each orbital were calculated using the density functional theory with the hybrid Becke three-parameter Lee-Yang-Parr (B3LYP) functional.[31] The standard correlation consistent basis set aug-cc-pVTZ was employed.[32] Theoretical momentum profiles were convolved with the experimental momentum resolution at the impact energy of 1200 eV using a Monte Carlo method.[33] The experimental intensities were rescaled by overlapping the maximum intensity of the calculated distributions and that of experimental distributions. The momentum distributions of each slice under different impact energies are displayed in Fig. 2 in comparison with the theoretical calculations. The distribution profiles at 1200 eV are the nearly same as that at 600 eV, which shows that PWIA is a good approximation in the present experiment. As shown in Figs. 2(a) and 2(c), the shapes of two slices of $3a_1$ do not have distinct difference at impact energies of 1200 and 600 eV. However, there are appreciable differences among the three slices of the 1*e* band in the low momentum region, which are presented in Figs. 2(b) and 2(d). In the low momentum region ($p < 0.2$ a.u.), the slices at the higher binding energies (17.1−17.9 eV) have higher intensities than those at the lower binding energies.

The differences among the momentum distributions of the selected slices in the 1*e* band are displayed more apparently in Figs. 3(b) and 3(d). The intensity ratio of the selected slices to the whole 1*e* band was plotted versus the momentum. For 1*e*, the whole band includes the intensity from 14.5 eV to 18.7 eV. For $3a_1$, the intensity in the binding energy range 9.7−12.3 eV was defined as the whole band. As shown in Figs. 3(b) and 3(d), the difference among the selected slices 17.1−17.9 eV, 15.1−5.9 eV, and 16.1−16.9 eV is noticeable in the low momentum region ($p < 0.3$ a.u.). There is a notable turn-up in the profile for 17.1−17.9 eV, while the profiles for 15.1− 5.9 eV and 16.1−16.9 eV hang down in this region. For the $3a_1$ band, the experimental ratios at different momenta fluctuate around the dotted line, as shown in Figs. 3(a) and 3(c). There is no evidently regular trend.

It is interesting to ask why the effects on the two orbitals are different. A possible reason is the vibronic coupling. The ionization from the non-degenerate $3a_1$ orbital only excites the umbrella vibrational mode. Removing an electron from the degenerate 1*e* orbital excites several vibrational modes intensively. To check the effects of different vibrational modes, geometries distorted by the vibration of NH_3^+ were used to calculate momentum distributions for the neutral non-equilibrium system, which is similar to the method used by Li *et al.*[23] and Tossell *et al.*[34] The cation NH_3^+ has a planar equilibrium geometry in its ground state. The ionization from the $3a_1$ orbital results in the umbrella mode ν_2 progression in the high resolution PES.[9,10,19] A series of geometries with displacements equal to α times the normalized vibrational eigen vector ($\alpha = 0, \pm 0.35, \pm 0.7$) were used to investigate the influence on the momentum distributions. The normalized vibrational eigen vector was defined as that its norm equals to

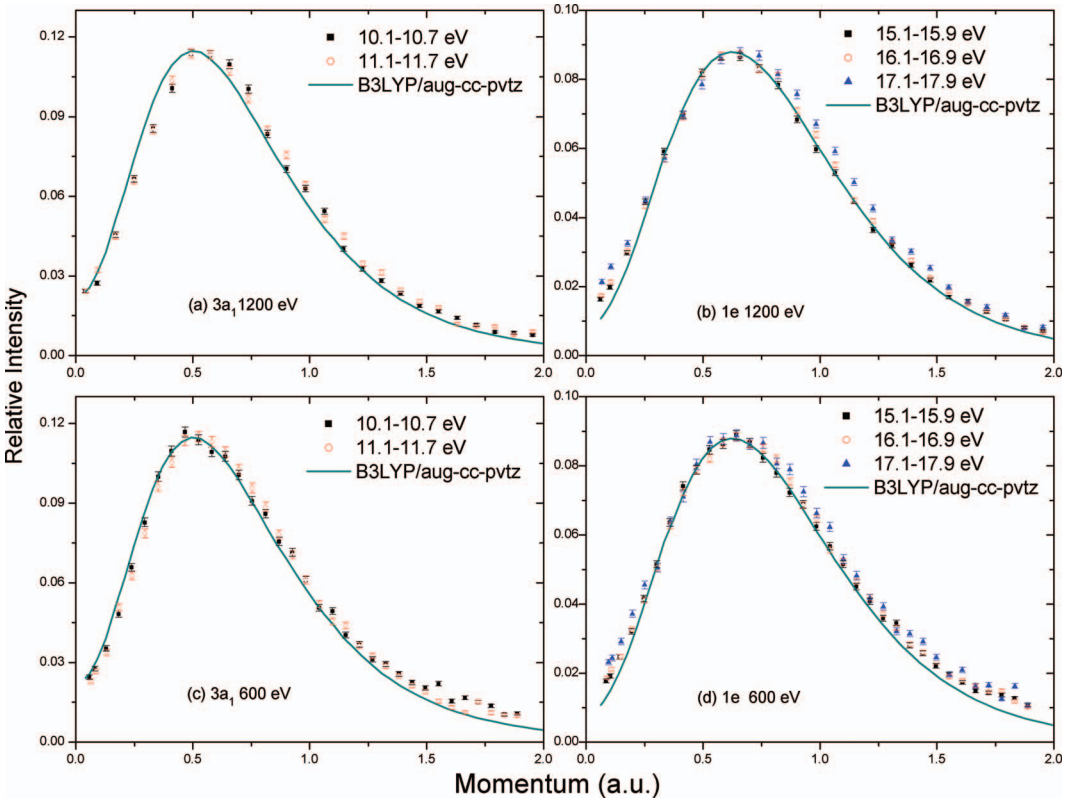

FIG. 2. Electron-momentum distributions of the different slices of $3a_1$ and $1e$ bands. The experimental distributions are compared with the B3LYP/aug-cc-pVTZ calculations. The experimental momentum resolution has been convolved in the calculation. (a) Momentum distributions of the two slices of $3a_1$ band under 1200 eV. (b) Momentum distributions of the three different slices of $1e$ band under 1200 eV. (c) Momentum distributions of the two slices of $3a_1$ band under 600 eV. (d) Momentum distributions of the three slices of $1e$ band under 600 eV.

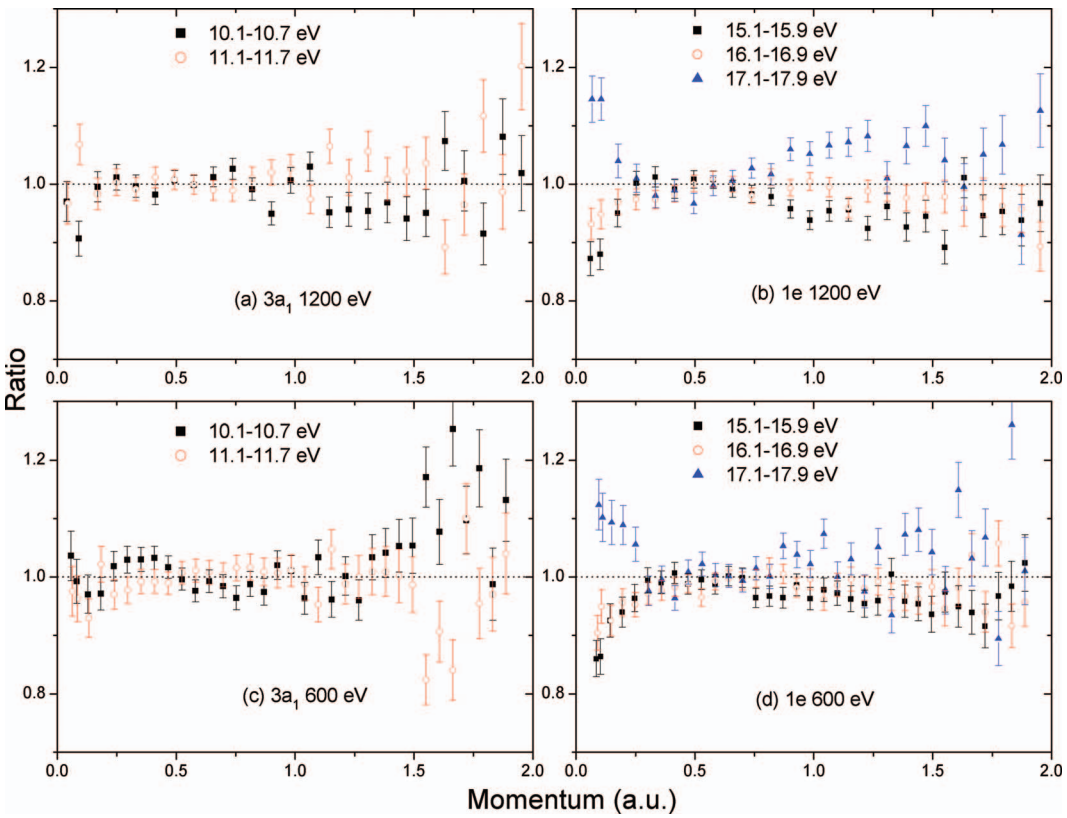

FIG. 3. The intensity ratios of the selected slices to the whole bands plotted versus the momentum (a) for $3a_1$ orbital under the impact energy of 1200 eV, (b) for $1e$ band under 1200 eV, (c) for $3a_1$ band under 600 eV, and (d) for $1e$ band under 600 eV. The error bars stand for one standard deviation.

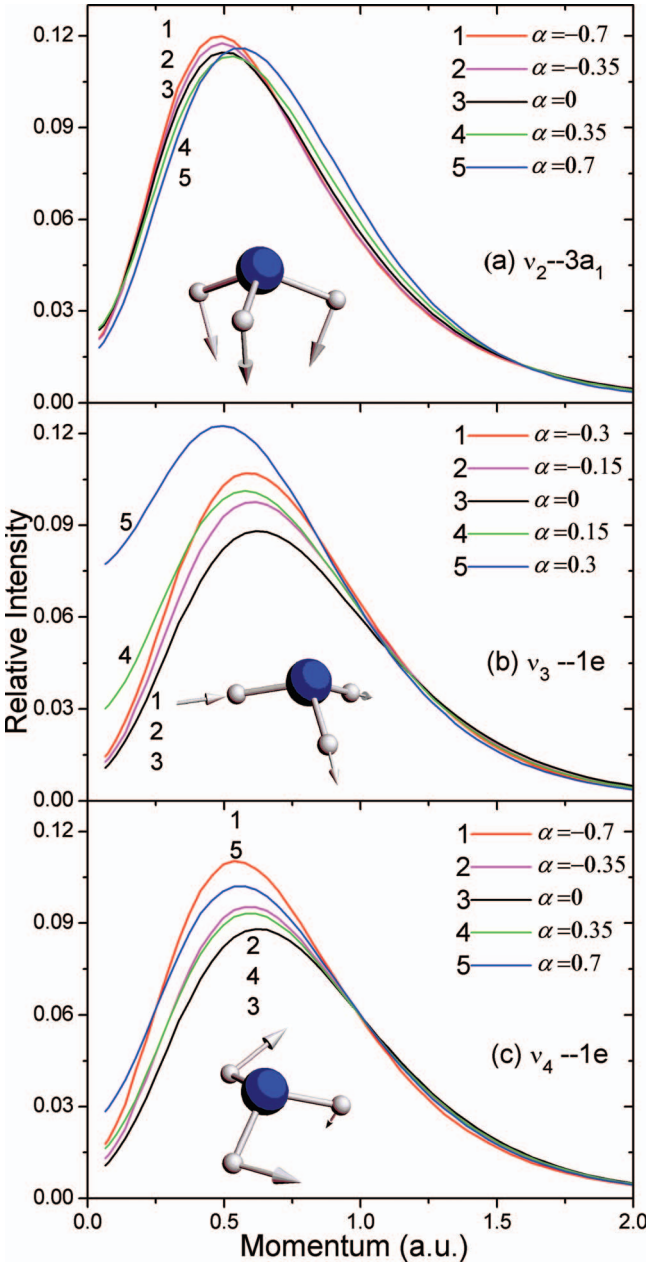

FIG. 4. The influence of geometry distortion along the vibrational modes upon the electron-momentum distributions of the $3a_1$ and $1e$ orbitals of NH_3. The profiles have been convolved with the experimental momentum resolution under the impact energy 1200 eV. (a) Momentum distributions of the $3a_1$ orbital for the umbrella mode ν_2. (b) Momentum distributions of the $1e$ orbital for the asymmetric stretching mode ν_3. (c) Momentum distributions of the $1e$ orbital for the bending mode ν_4. See text for the definition of the scaled displacement α. The displacement vectors of the nitrogen atoms are too small to display on the ammonia molecule models.

1 Å^2. The maximum displacement with a value of $\alpha = 0.7$ corresponding to an increase of 1.5 eV to the total energy of the cation ground state was determined by the vibrational broadening in the high resolution PES.[19] The total energy difference was calculated with the B3LYP/Aug-cc-pVTZ method. As shown in Fig. 4(a), the change of the theoretical momentum distributions is very small. This can roughly explain why we cannot observe differences between the two slices of $3a_1$ band in Figs. 3(a) and 3(c). The momentum distribution of the $3a_1$ orbital is insensitive to the ν_2 vibrational mode.

For the $1e$ band, Haller *et al.* showed that it is dominated by the strong Jahn-Teller activity of the asymmetric stretching mode ν_3 and the bending mode ν_4.[3] The theoretical momentum distributions with different displacements related to the two modes were shown in Figs. 4(b) and 4(c), respectively. Unlike the umbrella mode ν_2, the two vibronic modes remarkably change the momentum distributions, especially the asymmetric stretching mode ν_3. The deviations from the equilibrium geometry, no matter what the sign of α is, all result in the higher intensities in the low momentum region for both modes. This can partly explain the phenomena in Fig. 3. Compared with the slice in 15.1−15.9 eV, the slice in 17.1−17.9 eV is mainly contributed from the ionization where the cation was excited to a higher vibrational state. The more violent vibration will increase the intensity in the low momentum region more notably. As a result, there is a turn-up in Figs. 3(b) and 3(d).

From the comparison of $3a_1$ and $1e$ bands in Figs. 3 and 4, it is reasonable to conclude that the observed difference in the momentum distributions of the different slices of $1e$ band was due to the Jahn-Teller effects. The accurate calculation of the Jahn-Teller effect on the electron momentum distribution is still a challenge by far. Since NH_3 is one of the prototype molecules of Jahn-Teller effect, present experimental data will be a test bed for the future theoretical calculations of Jahn-Teller effect on the electron momentum distribution.

IV. CONCLUSIONS

The electron-momentum distributions of several nonadjacent slices in the two outer valence orbitals of NH_3 have been studied under impact energies of 1200 and 600 eV. For the $3a_1$ orbital, the momentum distributions of the two selected slices display no observable difference. But for the $1e$ band, there are notable differences among the momentum distributions of the three slices in the low momentum region, which reveals that the Jahn-Teller effect indeed influences on the electron momentum distribution of ammonia molecule.

ACKNOWLEDGMENTS

This work was supported by the National Nature Science Foundation of China (Grants No. 11074144 and 11174175).

[1] J. W. Rabalais, L. Karlsson, L. O. Werme, T. Bergmark, and K. Siegbahn, J. Chem. Phys. **58**, 3370 (1973).
[2] H. Koppel, L. S. Cederbaum, W. Domcke, and W. V. Niessen, Mol. Phys. **35**, 1283 (1978).
[3] E. Haller, L. S. Cederbaum, W. Domcke, and H. Koppel, Chem. Phys. Lett. **72**, 427 (1980).
[4] A. R. Rossi and P. Avouris, J. Chem. Phys. **79**, 3413 (1983).
[5] I. B. Bersuker, *The Jahn-Teller Effect and Vibronic Interactions in Modern Chemistry* (Plenum, New York, 1984).
[6] C. Krier, M. T. Praet, and J. C. Lorquet, J. Chem. Phys. **82**, 4073 (1985).
[7] J. M. Allen, M. N. R. Ashfold, R. J. Stickland, and C. M. Western, Mol. Phys. **74**, 49 (1991).
[8] I. B. Bersuker, Chem. Rev. **101**, 1067 (2001).
[9] C. Woywod, S. Scharfe, R. Krawczyk, W. Domcke, and H. Koppel, J. Chem. Phys. **118**, 5880 (2003).

[10]A. Viel, W. Eisfeld, S. Neumann, W. Domcke, and U. Manthe, J. Chem. Phys. **124**, 214306 (2006).
[11]D. W. Turner, C. Baker, A. D. Baker, and C. R. Brundle, *Molecular Photoelectron Spectroscopy* (Wiley, London, 1970).
[12]A. W. Potts and W. C. Price, Proc. R. Soc. London, Ser. A **326**, 181 (1972).
[13]M. S. Banna and D. A. Shirley, J. Chem. Phys. **64**, 4759 (1975).
[14]K. Kimura, S. Katsumata, Y. Achiba, T. Yamazaki, and S. Twata, *Handbook of He I Photoelectron Spectra of Fundamental Organic Molecules* (Halsted, New York, 1981).
[15]H. Argen, I. Reineck, H. Veenhuizen, R. Maripuu, R. Arneberg, and L. Karlsson, Mol. Phys. **45**, 477 (1982).
[16]G. Bieri, L. Asbrink, and W. von Niessen, J. Electron Spectrosc. Relat. Phenom. **27**, 129 (1982).
[17]M. N. Piancastelli, C. Cauletti, and M. Y. Adam, J. Chem. Phys. **87**, 1982 (1987).
[18]R. Locht, K. Hottmannn, and G. Hagenow, Chem. Phys. Lett. **190**, 124 (1992).
[19]D. Edvardsson, P. Baltzer, L. Karlsson, B. Wannberg, D. M. P. Holland, D. Shaw, and E. E. Rennie, J. Phys. B **32**, 2583 (1999).
[20]I. E. McCarthy and E. Weigold, Rep. Prog. Phys. **54**, 789 (1991).
[21]M. A. Coplan, J. H. Moore, and J. P. Doering, Rev. Mod. Phys. **66**, 985 (1994).
[22]E. Weigold and I. E. McCarthy, *Electron Momentum Spectroscopy* (Kluwer/Plenum, New York, 1999).
[23]Z. J. Li, X. J. Chen, X. Shan, T. Liu, and K. Z. Xu, J. Chem. Phys. **130**, 054302 (2009).
[24]J. R. Vanhise and D. N. McDonald, J. Chem. Phys. **61**, 2339 (1974).
[25]R. Camilloni, G. Stefani, A. Giardiniguidoni, R. Tiribelli, and D. Vinciguerra, Chem. Phys. Lett. **41**, 17 (1976).
[26]A. O. Bawagan and C. E. Brion, Chem. Phys. Lett. **137**, 573 (1987).
[27]A. O. Bawagan, R. Mullerfiedler, C. E. Brion, E. R. Davidson, and C. Boyle, Chem. Phys. **120**, 335 (1988).
[28]C. G. Ning, J. K. Deng, G. L. Su, H. Zhou, and X. G. Ren, Rev. Sci. Instrum. **75**, 3062 (2004).
[29]X. G. Ren, C. G. Ning, J. K. Deng, S. F. Zhang, G. L. Su, F. Huang, and G. Q. Li, Rev. Sci. Instrum. **76**, 063103 (2005).
[30]C. G. Ning, S. F. Zhang, J. K. Deng, K. Liu, Y. R. Huang, and Z. H. Luo, Chin. Phys. B **17**, 1729 (2008).
[31]C. Lee, W. Yang, and R. G. Parr, Phys. Rev. B **37**, 785 (1988).
[32]T. H. Dunning, J. Chem. Phys. **90**, 1007 (1989).
[33]P. Duffy, M. E. Casida, C. E. Brion, and D. P. Chong, Chem. Phys. **159**, 347 (1992).
[34]J. A. Tossell, J. H. Moore, and M. A. Coplan, Chem. Phys. Lett. **67**, 356 (1979).